

Article

# Lattice Wind Description and Characterization of Mexico City Local Wind Events in the 2001–2006 Period

Alejandro Salcido <sup>1,\*</sup>, Susana Carreón-Sierra <sup>1,†</sup>, Teodoro Georgiadis <sup>2,†</sup>,  
Ana-Teresa Celada-Murillo <sup>1,†</sup> and Telma Castro <sup>3,†</sup>

<sup>1</sup> Instituto de Investigaciones Eléctricas, División de Energías Alternas, Reforma 113, Palmira, Cuernavaca 62490, Mexico; E-Mails: susana.carreon@iie.org.mx (S.C.-S.); atcelada@iie.org.mx (A.-T.C.-M.)

<sup>2</sup> IBIMET-CNR, National Research Council of Italy, Institute of BioMeteorology, Bologna Section. Via Gobetti 101, Bologna 40129, Italy; E-Mail: t.georgiadis@ibimet.cnr.it

<sup>3</sup> Centro de Ciencias de la Atmósfera, Universidad Nacional Autónoma de México, Circuito Exterior, Ciudad Universitaria, Mexico, D.F. 04510, Mexico; E-Mail: telma@atmosfera.unam.mx

<sup>†</sup> These authors contributed equally to this work.

\* Author to whom correspondence should be addressed; E-Mail: salcido@iie.org.mx; Tel.: +52-777-362-3811 (ext. 7087).

Received: 26 May 2015 / Accepted: 21 July 2015 / Published: 31 July 2015

---

**Abstract:** Urban transformation and expansion in Mexico City continuously affect its urban morphology, and therefore the modes of wind circulation inside it and their occurrence probabilities. Knowledge on these topics is an important issue for urban planning and for other urban studies, such as air quality assessment. In this paper, using a lattice wind model at a meso- $\beta$  scale, we develop a simple description and characterization of Mexico City local wind events that occurred during the period 2001–2006, including an estimation of the occurrence probabilities. This region was modeled as a 2D lattice domain of identical cells, and wind conditions in each cell were described by four wind attributes: the horizontal velocity components, divergence, and vorticity. Models of one and four cells were applied to wind data furnished by the meteorological network of the city. Results include the following: Early morning: low intensity winds (75%) from N, NW, W and SW (75%), convergent (93%), with a slight predominance of cyclonic vorticity (54%). Morning and early afternoon: winds from N, NE and E (72%) with speeds from 0.5 to 3.5 m/s, slight prevailing of convergent winds (51%), and slight predominance of cyclonic vorticity (57%).

Late afternoon and night: winds blowing from N, NW, and S (63%) with speeds from 1.5 to 3.5 m/s (66%), convergent (90%), and cyclonic (72%).

**Keywords:** urban local wind; lattice wind model; Mexico City

---

## 1. Introduction

In this paper, we performed a wind taxonomy study of Mexico City for the period 2001–2006. Our main objective was to identify and characterize the local wind events of the city and estimate their occurrence probabilities. This study was carried out from the standpoint of a lattice wind model (LWM) at a meso- $\beta$  scale [1–3] using the wind data measured by the meteorological network (REDMET) of the atmospheric monitoring system (SIMAT) for the Mexico City Metropolitan Area [4]. The LWM yields a set of model wind events (or wind states) which are described individually in terms of four continuous state parameters, the horizontal wind velocity components ( $u$ ,  $v$ ), the wind divergence ( $\gamma$ ), and the wind vorticity ( $\omega$ ). In this paper, however, the statistical analysis of the Mexico City model wind events was carried out in terms of the finite set of discrete wind states that results from using simple discrete scales of measurement to assign their values to the state parameters. This analysis provides a characterization of the wind states and an estimation of their occurrence probabilities from an individual standpoint. In another paper [5], otherwise, we studied the same set of continuous wind states from the standpoint of hierarchical cluster analysis with the purpose of recognizing and characterizing the clusters of wind states that can be considered as instances or cases of the wind circulation patterns that prevailed in the Mexico City region during the period 2001–2006.

Description and characterization of the local wind events and the estimation of their occurrence probabilities are important issues for different purposes in several fields of application, such as urban planning, wind resource assessment, and air quality assessment, among others. Increasing urban transformation and expansion change the morphology of a city, and these modifications have to be taken into account in urban planning because they induce mechanical and thermal processes that change the local wind circulation conditions [6], affect the local urban climate [7], and intensify the urban heat island [8–10]. During air quality assessment, knowing the wind circulation modes in a city allows one to understand how the emissions of pollutants will be transported and dispersed in the atmosphere [11,12], how these emissions will impact the area near the sources [13], and how to evaluate the possibilities of pollution being transported toward the surrounding urban and rural settlements [14]. On the other hand, an accurate wind resource assessment, the process by which wind power developers estimate the future energy production of a wind farm, requires knowledge of the main wind circulation scenarios which are crucial to the successful development of urban wind farms [15].

### 1.1. The Study Region

Mexico City lies inside the tropical Basin of Mexico, located in the middle region of the neovolcanic axis (between 19.0 and 19.6 degrees north latitude and 98.9 and 99.4 degrees west longitude). It has an average altitude of 2240 m and is almost completely surrounded by high mountains, with only two main

openings located at the south and the north sides of the basin. Figure 1 shows an altitude profile of the mountains that surround the Mexico City basin. It was prepared following the perimeter drawn in the figure at right, clockwise from the left top vertex. This profile shows that the main ventilation possibilities of Mexico City are associated with the eastern wind channel crossing south-north the Mexico Basin. This feature favors northerly, northeasterly and southerly wind circulation, driven by synoptic winds and temperature gradients. However, due to the mountain-valley system of Mexico City, drainage winds are also driven systematically, mainly during nighttime and early morning, and frequently reinforced by the urban heat island phenomenon [9,10].

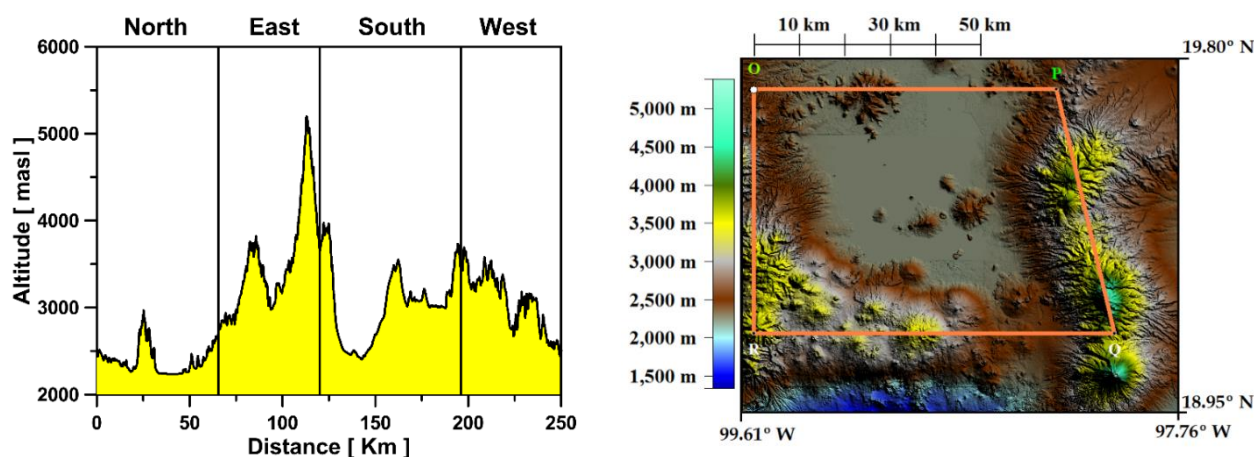


**Figure 1.** Altitude profile (left) of the mountains that surround the Mexico City basin (right).

### 1.2. About the Study Period

The continuous transformation and expansion of the MCMA affects its urban morphology, and therefore the modes of surface wind circulation inside it. During the period 2001–2006, within the framework of a Latin American trend to return to central urban areas, the local government conducted several urban housing and rescuing policies related to the heritage of Mexico City's historic center [16]. Moreover, in the same period, within the framework of an integral public transportation and highway administration program [17], the local government carried out the construction of cultural and touristic corridors, strategic corridors for public transportation, vehicular traffic corridors, the second floors over Viaducto and Periferico freeways [18,19], vehicular bridges, and some other urban structures. In this period, the growth rate of urbanized area was 495 ha per year, while the loss rate for ecological reserves was 400 ha per year [20]. All these initiatives and processes impacted Mexico City's urban morphology, and therefore the wind circulation in the city, and also affected the performance of its ventilation mechanisms.

During the period 2001–2006, at least three important field measurement campaigns were executed in the MCMA. Throughout 2001, the M4CA group of the Instituto de Investigaciones Eléctricas carried out the first long-term surface micrometeorological campaign (IIE2001) in Mexico City with the economic support of the Consejo Nacional de Ciencia y Tecnología (CONACyT) and technical assistance from Italian institutions (Servizi territorio srl and IBIMET-CNR) [21]. During the spring of 2003 (1 April–5 May), the MCMA-2003 Field Measurement Campaign was performed by a multinational team of experts led by Luisa Molina of MIT [22]. Also, the Megacity Initiative: Local and Global Research Observations

(MILAGRO) project brought an international research team of scientists and collaborating Mexican government agencies to the Mexico City area and Veracruz in March 2006 [23]. The goal of MILAGRO was to conduct measurements of pollutants and aerosol particles, and to study the atmospheric processes leading to the formation of secondary aerosols from precursor gases and the transport and transformations of these gases and aerosols on local, regional, and global scales. The overall goals of all these efforts have been contributed to the understanding of the air quality problem in megacities by conducting measurements and modeling studies of atmospheric pollutants in the MCMA [22]. Because of these international initiatives, the period 2001–2006 represents an historical and very interesting opportunity for the investigation of the air pollution problems of Mexico City.

Though REDMET (SIMAT) started its operation in 1986 with ten meteorological stations, it reached a consolidated state up to 2001 after the installation of five new stations in the course of year 2000. During the period 2001–2006, the number of stations of REDMET remained fixed, and the data processing and organization of the databases remained quite stable. However, one of the old stations (Hangares) went out of operation completely in 2006. New stations were incorporated in 2007 and 2008, and hereafter important modifications were made in relation with the organization of the databases.

### 1.3. Material Organization

The material of rest of this paper is organized as follows. In Section 2, the general methodological aspects of the study are presented. This section includes a brief description of the lattice wind modeling approach that we followed to model the Mexico City local wind events, emphasizing the main concepts of wind state (WS), discrete wind state (DWS), and wind direction state (WDS) that we used to describe the model wind events. In Section 3, the principal results derived from this wind taxonomy study are presented and discussed. Here, in Section 3.1, the temporal behavior of the model wind events and the statistics of the wind state parameters during the period 2001–2006 are presented; in Section 3.2, the characteristics and occurrence probabilities of the model wind events are analyzed and discussed in terms of the set of discrete wind states that results when the continuous wind state parameters are expressed in terms of some given discrete and finite measurement scales; in Section 3.3, the concept of wind direction state is applied to illustrate the principal modes of wind circulation in Mexico City during the study period, including an estimation of their occurrence probabilities. Finally, in Section 4, the principal conclusions of this work are summarized.

## 2. Methodological Framework: the Lattice Wind Modeling Approach

Mexico City is modeled as a 2D lattice domain of identical rectangular cells. The local wind condition at each cell is assumed to be described by the spatial averages over the cell of the wind velocity components ( $u$ ,  $v$ ), the wind divergence  $\gamma$ , and the wind vorticity  $\omega$ . The quartet ( $u$ ,  $v$ ,  $\gamma$ ,  $\omega$ ) represents the *wind state* (WS) at a lattice cell (that is, a model local wind event at the cell). The set of the wind states that one can observe is determined by the topographical features of the region in conjunction with all other wind driving forces prevailing there. Here, divergence and vorticity are included as additional wind state variables; this endows the model with a slightly non-local character and consents to recover one part of the wind information lost by the filtering effect of the spatial averaging processes. Afterward, from the standpoint of a lattice wind model (LWM), it is assumed that the mean velocity and its mean

tendencies of rotation and divergence are known at each cell. Obviously, each wind state can be described also by a quartet ( $U, \theta, \gamma, \omega$ ), where  $U$  and  $\theta$  denote the speed and direction of the mean wind velocity.

In this work we followed a very simple procedure to estimate Mexico City's wind states. We applied a Kriging vector interpolation technique (boundary-constrained) to the wind data of the meteorological network REDMET (SIMAT) of Mexico City to estimate the wind velocity components ( $u, v$ ) at the 81 nodes of an  $9 \times 9$  calculation grid, which was selected to completely cover the region of interest. These estimations of ( $u, v$ ) were used to calculate the spatial average parameters ( $u, v, \gamma, \omega$ ) at the cells of the  $8 \times 8$  lattice associated with the calculation grid, using their 2D numerical definitions [24]:

$$\text{Wind Velocity} \quad u(i, j) = \frac{1}{4} [u_{(r,s)} + u_{(r+1,s)} + u_{(r,s+1)} + u_{(r+1,s+1)}] \quad (1)$$

$$\text{Components:} \quad v(i, j) = \frac{1}{4} [v_{(r,s)} + v_{(r+1,s)} + v_{(r,s+1)} + v_{(r+1,s+1)}] \quad (2)$$

$$\begin{aligned} \text{Wind} \quad \gamma(i, j) &= \frac{1}{2\Delta x} \{ [u_{(r+1,s+1)} - u_{(r,s+1)}] + [u_{(r+1,s)} - u_{(r,s)}] \} \\ \text{Divergence:} \quad &+ \frac{1}{2\Delta y} \{ [v_{(r+1,s+1)} - v_{(r+1,s)}] + [v_{(r,s+1)} - v_{(r,s)}] \} \end{aligned} \quad (3)$$

$$\begin{aligned} \text{Wind} \quad \omega(i, j) &= \frac{1}{2\Delta x} \{ [v_{(r+1,s+1)} - v_{(r,s+1)}] + [v_{(r+1,s)} - v_{(r,s)}] \} \\ \text{Vorticity:} \quad &- \frac{1}{2\Delta y} \{ [u_{(r+1,s+1)} - u_{(r+1,s)}] + [u_{(r,s+1)} - u_{(r,s)}] \} \end{aligned} \quad (4)$$

With reference to Figure 2, these equations provide a simple estimation of the wind state parameters at the central cell ( $i, j$ ) in terms of the velocity components ( $u, v$ ) at its four neighboring grid nodes ( $r, s$ ). Here  $\Delta x$  y  $\Delta y$  are the distances between adjacent nodes in the  $x$  and  $y$  directions, respectively.

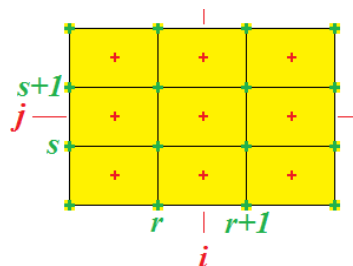


**Figure 2.** Arrangement of a centered finite differences grid.

Then, the estimations of the wind state parameters ( $u, v, \gamma, \omega$ ) at the 64 ( $i, j$ )-cells of the calculation grid were used to calculate their spatial averages over each cell of the LWM of Mexico City. LWMs with 1 and 4 cells were taken into account.

The spatial domain was the portion of Mexico City located at  $19.30$ – $19.57$  °N and  $99.00$ – $99.27$  °W. This region is the (unique) cell when the 1-cell model is applied to Mexico City. The same region is considered to be divided into the quadrants NE, NW, SW and SE when the 4-cell LWM is applied. The cells or city quadrants are defined with reference to the origin located at the point ( $99.134$  °W,  $19.433$  °N), which is the geometric centroid of the REDMET stations. The quadrants were  $14.0$  km long in the west-east direction, and  $18.5$  km long in the south-north direction. The spatial resolution of the calculation grid was  $3.11$  km in the west-east direction and  $4.11$  km in the south-north direction. Figure 3 shows the lattice domains, and Table 1 summarizes the positions of the centers of the city quadrants.

**Table 1.** Geographical positions of the centers of the Mexico City quadrants.

City Quadrant	Latitude (° N)	Longitude (° W)
NE	19.499	99.067
NW	19.499	99.200
SW	19.366	99.200
SE	19.366	99.067

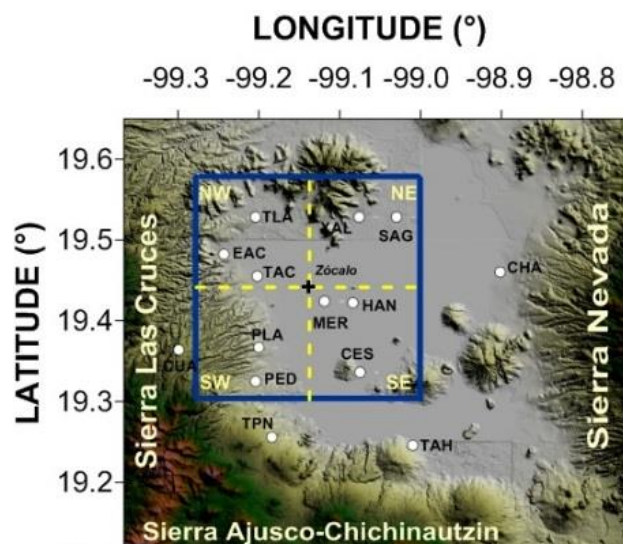
**Figure 3.** The lattice domain. The blue solid rectangle represents the cell of the 1-cell LWM of Mexico City. The quadrants defined by the solid line rectangle divided by dashed lines represent the cells of the 4-cell LWM. Positions (white solid circles) and IDs of the REDMET stations are also shown.

Table 2 summarizes the average availability of wind data of the meteorological stations of the REDMET in the period 2001–2006. For future reference, this table include also the IDs of the stations.

**Table 2.** Average availability of wind data at the REDMET stations in the period 2001–2006.

REDMET Stations	ID	Valid Data (%)
Tacuba	TAC	95
ENEP Acatlán	EAC	93
San Agustín	SAG	66
Tlanepantla	TLA	91
Xalostoc	XAL	93
Merced	MER	93
Pedregal	PED	95
Cerro de la Estrella	CES	90
Plateros	PLA	93
Hangares	HAN	79
Villa de las Flores	VIF	90
Cuajimalpa	CUA	89
Tlalpan	TPN	45
Chapingo	CHA	89
Tlahuac	TAH	84

The performances of San Agustin (SAG) and Tlalpan (TPN) stations were very low (the red cells in Table 2). They did not meet the data validation criteria of SIMAT and were excluded from the wind data base. The stations Villa de las Flores (VIF), Cuajimalpa (CUA), Chapingo (CHA), and Tlahuac (TAH) are located out of the spatial domain of study and they were excluded too (the green cells in Table 2).

### 2.1. Discrete Wind States

For some purposes, it is convenient to use discrete scales of measure to assign values to the wind state parameters; in this case the wind states are referred as *discrete wind states* (DWS). A DWS can be identified with a non-negative integer number  $\varepsilon$  given by

$$\varepsilon = \omega + S_{\omega}[\gamma + S_{\gamma}(\theta + S_{\theta}U)] \quad (5)$$

whenever the levels (or categories) of the discrete measuring scales are labeled by no-negative integers, and  $S_{\omega}$ ,  $S_{\gamma}$ , and  $S_{\theta}$  denote the numbers of discrete levels of wind vorticity, divergence, and direction, respectively. For the description purposes of the results, we used  $S_{\theta} = 8$  and  $S_{\omega} = S_{\gamma} = 3$ , with the categories 0, 1, 2, 3, 4, 5, 6, and 7 for wind direction, and 0, 1, and 2 for both wind divergence and wind vorticity, as defined in Table 3.

**Table 3.** Categories of the discrete scales of wind direction, divergence, and vorticity.

	N	NE	E	SE	S	SW	W	NW
	(North)	(Northeast)	(East)	(Southeast)	(South)	(Southwest)	(West)	(Northwest)
<b>Wind Direction</b>	↓	↗	←	↖	↑	↘	→	↙
	<b>0</b>	<b>1</b>	<b>2</b>	<b>3</b>	<b>4</b>	<b>5</b>	<b>6</b>	<b>7</b>
<b>Wind Divergence</b>	$\gamma < 0$	$\gamma = 0$	$\gamma > 0$		Wind Vorticity	$\omega < 0$	$\omega = 0$	$\omega > 0$
	<b>0</b>	<b>1</b>	<b>2</b>			<b>0</b>	<b>1</b>	<b>2</b>

Wind speed categories were assigned using the Beaufort scale. For reference, Table 4 shows the first six categories of this scale. With this notation, e.g., wind state 191 denotes  $(U, \theta, \gamma, \omega) = (3, 5, 0, 2)$ , which describes a wind event with intensity between 3.5 and 5.5 m/s, blowing from the SW, with convergent and cyclonic features.

**Table 4.** First six categories of the Beaufort scale.

Beaufort Category	ID	Description	Wind Speed Range (m/s)
0	B0	<i>Calm</i>	$0 \leq v < 0.25$
1	B1	<i>Light Air</i>	$0.25 \leq v < 1.5$
2	B2	<i>Light Breeze</i>	$1.5 \leq v < 3.5$
3	B3	<i>Gentle Breeze</i>	$3.5 \leq v < 5.5$
4	B4	<i>Moderate Breeze</i>	$5.5 \leq v < 8.0$
5	B5	<i>Fresh Breeze</i>	$8.0 \leq v < 10.7$

### 2.2. Wind Direction States

If the 4-cell LWM is used to describe Mexico City's wind circulation, a very simple illustration is obtained from the concept of wind direction state (WDS). Mexico City is represented by a  $2 \times 2$

rectangular lattice, where each cell represents a quadrant of the city. The wind conditions at the city quadrants are described by the quartets  $(U, \theta, \gamma, \omega)_{NE}$ ,  $(U, \theta, \gamma, \omega)_{NW}$ ,  $(U, \theta, \gamma, \omega)_{SW}$ , and  $(U, \theta, \gamma, \omega)_{SE}$ . Then, the WDS of the city is defined by the four wind directions,  $\theta_{NE}$ ,  $\theta_{NW}$ ,  $\theta_{SW}$ , and  $\theta_{SE}$ , of the mean wind velocities in the cells. If we express wind direction in terms of the 8-sectors scale (N, NE, E, SE, S, SW, W, NW), the WDS provides a very simple but illustrative pictorial view of the wind circulation in the city. In this case, the WDS is represented by a  $2 \times 2$  array of small squares (representing the city quadrants), each one with an arrow inside that indicates the wind direction in the cell according to Table 3. The WDS can be conveniently identified by a four-digit octal number (or by its decimal form), whose digits, from left to right, denote (Table 3) the wind direction in the city quadrants NE, NW, SW and SE, respectively.

### 2.3. Occurrence Probabilities of the Wind States

The occurrence frequency distribution of the wind states constitutes a convenient way to quantify the occurrence probabilities of the model wind events. For a given wind state, its occurrence frequency is the fraction of the number of times this wind state occurred, relative to the total number of wind events that occurred during the period of time of the study.

## 3. Results and Discussion

### 3.1. Mexico City Wind States (2001–2006)

From the standpoint of the 1-cell LWM, the temporal evolution of the wind circulation in Mexico City during the period 2001–2006 is described by the time series of the wind state parameters ( $u$ ,  $v$ ,  $\gamma$ ,  $\omega$ ) shown in Figure 4. The frequency distribution of the values of the wind state parameters are also shown in Figure 4, and their basic statistics are summarized in Table 5. This table also includes the statistics of wind speed (WSP). These results reflect the following remarkable characteristics of the Mexico City winds:

**Mean Wind Velocity Components:** The West-to-East wind component ( $u$ ) was positive for 52% of the hourly wind states, showing a slight predominance of winds from the west sectors of the city flowing to downtown. In turn, the South-to-North wind component ( $v$ ) was negative for 66% of the hourly wind states, which indicates a clear predominance of winds with a flow component from north. The intensity of the model wind events, in terms of the Beaufort scale categories, was as follows: 9% of the wind events were *calm*, the 65% were *light air*, and 26% were *light breeze*. Higher wind speed values were not reflected by the model wind events.

**Table 5.** Statistics of the wind state parameters. Period 2001–2006.

	$u$ (m/s)	$v$ (m/s)	WSP (m/s)	$\gamma$ ( $\times 10^{-4}$ 1/s)	$\omega$ ( $\times 10^{-4}$ 1/s)
Minimum	−4.99	−5.50	0.00	−4.46	−2.77
Maximum	4.82	5.17	5.89	3.78	4.17
Mean	0.03	−0.43	1.11	−0.55	0.21
Mode	0.14	0.02	0.42	−0.69	−0.15
Std. Dev.	0.67	1.16	0.86	0.70	0.59
Kurtosis	3.76	1.53	1.96	0.52	2.81
Skewness	0.42	−0.012	1.38	−0.16	0.95



**Mean Wind Divergence and Vorticity:** The wind divergence ( $\gamma$ ) was negative for 78% of the model wind events. This indicates that the convergent winds prevailed not only during the nighttime, but also during 50% of the daylight hours, just when one would be expecting that turbulent mixing would weaken the flow induced by the urban heat island [9,25]. The wind vorticity ( $\omega$ ), on the other hand, was positive during 61% of the wind events, indicating predominance of cyclonic winds. Given the regional topography, this fact could be partially correlated (at least) with the predominance of winds with a northerly flow component (66%).

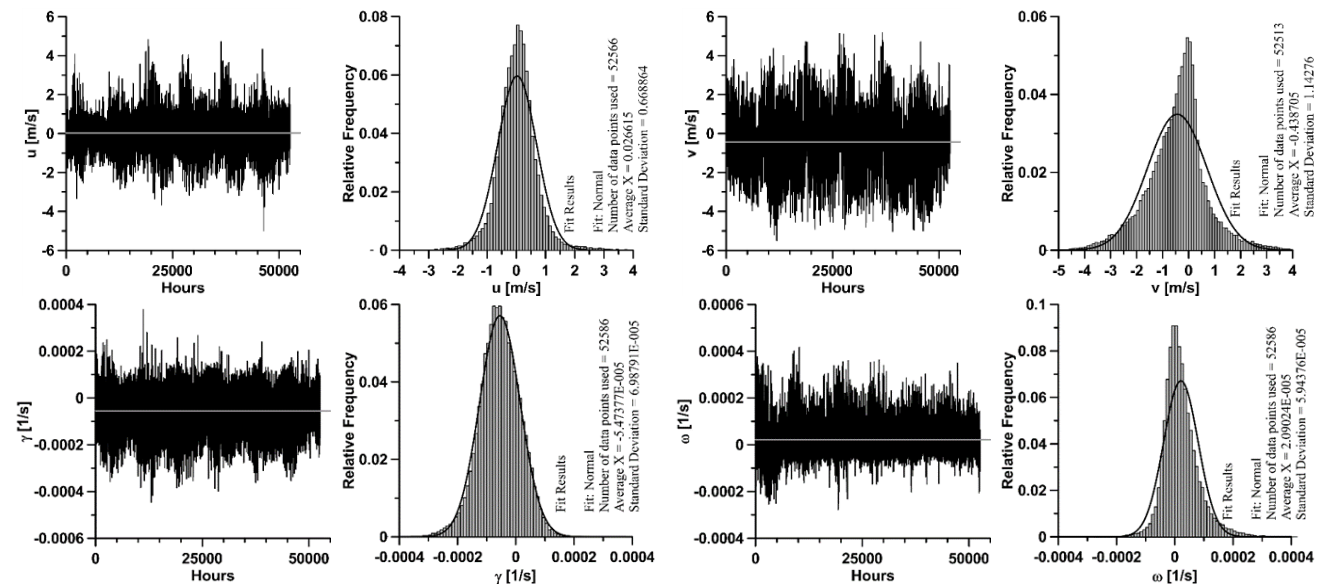


**Figure 4.** Temporal behavior (left) and frequency distribution (right) of the Mexico City wind state parameters during the period 2001–2006. Top row: velocity components ( $u$ ,  $v$ ). Bottom row: divergence ( $\gamma$ ) and vorticity ( $\omega$ ). Fittings to normal distributions are shown for comparison purposes.

The mean values presented in this table describe the mean winds of Mexico City: low intensity, northerly winds with slightly convergent and cyclonic features. This may be illustrated as in Figure 5.

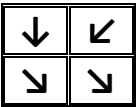


**Figure 5.** Schematic illustration of the mean wind circulation mode in Mexico City (2001–2006).

### 3.2. Mexico City Discrete Wind States (2001–2006)

On the other hand, Figure 6 and Table 6 summarize the results that we obtained for the occurrence frequencies of the discrete wind states (DWS) from the standpoint of the 1-cell model of Mexico City. Figure 6 shows that, in the period 2001–2006, Mexico City’s discrete wind states had intensities that belong almost exclusively to the second (B1, *light air*) and third (B2, *light breeze*) categories of the Beaufort scale. It is observed, in fact, that the first three DWSs with the highest frequencies appeared in the B2 category. Table 6 summarizes the first seventeen discrete wind states of Mexico City with the highest occurrence frequencies throughout 2001–2006. This set comprises the 62% of the discrete wind states

of the period. The one with highest occurrence frequency (10.96%) in the period was the 146 (2, 0, 0, 2). This state represents a northerly wind condition with intensities in the third category of Beaufort, and with convergent and cyclonic features. The DWS with the second highest occurrence frequency (5%) was that one identified as 144 (2, 0, 0, 0), which represents winds with the same characteristics as the 146, except the vorticity, which in this case is anticyclonic.

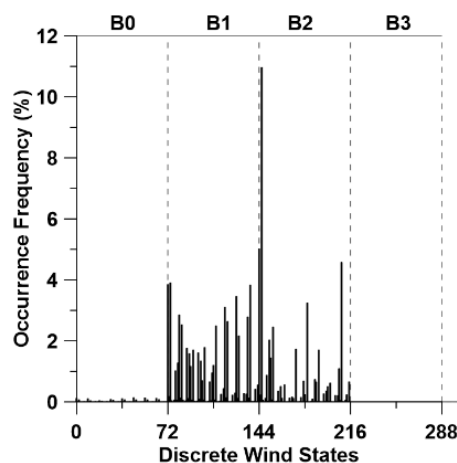


**Figure 6.** Distribution of the occurrence frequencies of the discrete wind states.

**Table 6.** Mexico City discrete wind states with the highest occurrence frequencies. Period: 2001–2006.

<i>ID</i>	<i>(U, θ, γ, ω)</i>	<i>Occurrences</i>	<i>Frequency (%)</i>	<i>WSP (m/s)</i>	<i>WDR</i>	<i>DIV</i>	<i>VOR</i>
146	( 2, 0, 0, 2)	5765	10.9634	$1.5 < v < 3.5$	N	Convergent	Cyclonic
144	( 2, 0, 0, 0)	2635	5.0110	$1.5 < v < 3.5$	N	Convergent	Anticyclonic
209	( 2, 7, 0, 2)	2405	4.5736	$1.5 < v < 3.5$	NW	Convergent	Cyclonic
74	( 1, 0, 0, 2)	2055	3.9080	$0.25 < v < 1.5$	N	Convergent	Cyclonic
72	( 1, 0, 0, 0)	2024	3.8491	$0.25 < v < 1.5$	N	Convergent	Anticyclonic
137	( 1, 7, 0, 2)	2013	3.8282	$0.25 < v < 1.5$	NW	Convergent	Cyclonic
126	( 1, 6, 0, 0)	1820	3.4611	$0.25 < v < 1.5$	W	Convergent	Anticyclonic
182	( 2, 4, 0, 2)	1706	3.2443	$1.5 < v < 3.5$	S	Convergent	Cyclonic
117	( 1, 5, 0, 0)	1631	3.1017	$0.25 < v < 1.5$	SW	Convergent	Anticyclonic
81	( 1, 1, 0, 0)	1499	2.8507	$0.25 < v < 1.5$	NE	Convergent	Anticyclonic
135	( 1, 7, 0, 0)	1466	2.7879	$0.25 < v < 1.5$	NW	Convergent	Anticyclonic
119	( 1, 5, 0, 2)	1389	2.6415	$0.25 < v < 1.5$	SW	Convergent	Cyclonic
83	( 1, 1, 0, 2)	1332	2.5331	$0.25 < v < 1.5$	NE	Convergent	Cyclonic
110	( 1, 4, 0, 2)	1312	2.4951	$0.25 < v < 1.5$	S	Convergent	Cyclonic
155	( 2, 1, 0, 2)	1290	2.4532	$1.5 < v < 3.5$	NE	Convergent	Cyclonic
128	( 1, 6, 0, 2)	1139	2.1661	$0.25 < v < 1.5$	W	Convergent	Cyclonic
152	( 2, 0, 2, 2)	1068	2.0310	$1.5 < v < 3.5$	N	Divergent	Cyclonic

As shown in Table 6, the main wind directions of the wind states were N (5/17), NW (3/17), and NE (3/17), and after that SW (2/17) and W (2/17). Their absolute occurrence frequencies were 30%, 15%, 14%, 10% and 8%, respectively. Almost all these wind states represented convergent winds (16/17). It is also shown that the discrete wind states with cyclonic vorticity were the majority (11/17) in this set.

Moreover, the states representing winds with intensity in the second category of Beaufort (*light air*) were also in the majority (11/17), while the rest (6/17) were *light breezes* (winds with intensity in the third category of Beaufort). No wind states representing *calms*, neither wind states with intensities in the higher categories of Beaufort were found in this set. Table 7 summarizes the absolute fractions of the DWSs with some specific discrete values of the wind state parameters. These results indicate that the local winds in Mexico City during the period 2001–2006 were blowing mainly (59%) from the north sectors (NW, N, and NE) of the city, with low intensities (9% *calms*, 65% *light air*, 24% *light breeze*, and 2% *gentle breeze*), and with convergent (78%) and cyclonic (61%) features.

**Table 7.** Percentages (%) of the wind events for each discrete value of the wind parameters.

WSP: Beaufort Categories				Wind Direction								DIV < 0	VOR > 0
B0	B1	B2	B3	N	NE	E	SE	S	SW	W	NW		
9	65	24	2	30	14	7	7	9	10	8	15	78	61

On the other hand, in order to obtain a better description of wind behavior in Mexico City throughout the day, the set of discrete wind states was partitioned and organized into three subsets according to their occurrence hours: early morning (00–07 CST), morning and early afternoon (08–15 CST), and late afternoon and night (16–23 CST). The hour ID (00, 01, 02 ...) denotes the beginning of 1 h averaging period of the original wind data. These time windows were selected according to the following criteria. Let us consider Figure 7. It shows the annual average of the hourly trends of global solar radiation, temperature, and wind speed that were measured in three sites of Mexico City during the first long-term surface micrometeorological campaign (IIE2001) carried out in this region throughout the year 2001 [21]. The measuring sites, called Texcoco (TEX), Azcapotzalco (AZC), and Xochimilco (XOC), were located in the NE, NW and SE quadrants of the city (Table 8).

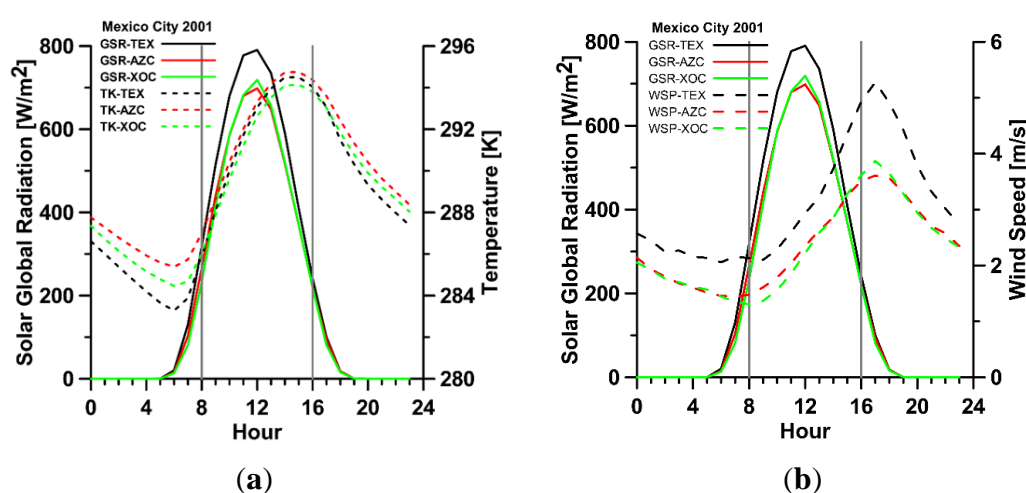


**Figure 7.** Annual averages of the hourly trends of global solar radiation (GSR), temperature (TK), and wind speed (WSP) measured in Mexico City at the stations Texcoco (TEX), Azcapotzalco (AZC) and Xochimilco (XOC) during the IIE2001 campaign [21].

**Table 8.** Micrometeorological stations of the IIE2001 campaign.

Station	ID	Quadrant	Latitude (N)	Longitude (W)	Altitude (masl)
Texcoco	TEX	NE	19 °27' 53.1"	98 °59' 54.4"	2250
Azcapotzalco	AZC	NW	19 °30' 9.4"	99 °11' 12.2"	2190
Xochimilco	XOC	SE	19 °18' 18.3"	99 °6' 6.2"	2250

According to this figure, the first time window (early morning) starts at midnight and finishes two hours after sunrise; this is the coldest period of the day (Figure 7a), as the temperature decreases from 287 to a minimum of 285 K at sunrise (6:30h CST). As shown in Figure 7b, a slow decrease in wind speed (with values around 2 m/s) is observed during this period, and it reaches its minimum value around hour 8. Of course, it is expected that fully developed katabatic winds will be observed driven by the Mexico City mountain-valley system during these hours. The second time window (morning and early afternoon) comprises the main part of the daylight hours, starting after sunrise and finishing two hours before sunset; this is the period of maximum solar irradiance and temperature grows and reaches its maximum around hour 15 of the day (Figure 7a), while wind speed increases and reaches its maximum value around hour 17 (Figure 7b). It can be expected that prevailing local winds in this period are driven by the synoptic circulation and the temperature gradients between the city and its surroundings, also reflecting the effect of the South-North wind channel located at the east side of the city (Figure 1). The third time window (late afternoon and night) starts one or two hours before sunset and finishes at midnight. This is the cooling period of the day; the global solar radiation drops to zero between hours 18 and 19, temperature decreases from 295 to 288 K (Figure 7a) and wind speed quickly decreases from 5.5 m/s to 2 m/s, approximately (Figure 7b). During this period, wind behavior is expected that reflects the superposing of the remaining gap winds of the late afternoon with the start of katabatic wind development, especially close to the mountains located at the west side of the city. These observations suggest that a partition of the day into time windows 8 h long could be appropriate for analyzing the time behavior of Mexico City winds, at least as a first approximation.

Graphs (a), (b), and (c) in Figure 8 show the occurrence frequencies of the discrete wind states that belong to the subsets identified by the time windows defined above. The occurrence frequency distributions shown in these figures reflect, qualitatively, the same general features of wind speed shown in Figure 7b.

Table 9 summarizes the percentages of wind events (relative to the total number of 52,584 events) that occurred, with some specific discrete values of the wind parameters for the same 8h-periods. This table, in terms of the percentages relative to the number of events of the 8h-period over 6 years (17,528), shows that the prevailing winds had the following characteristics: Early morning (00-07 CST): Winds were convergent (93%), had intensities from 0.25 to 1.5 m/s (75%), and were blowing from N, NW, W and SW (75%) with a slight predominance of cyclonic vorticity (54%). Morning and early afternoon (08-15 CST): Winds were blowing from N, NE and E (72%), had intensities from 0.5 to 3.5 m/s, and revealed a slight predominance of convergence (51%) and cyclonic vorticity (57%). Late afternoon and night (16-23 CST): Winds were convergent (90%) and cyclonic (72%), had intensities from 1.5 to 3.5 m/s (66%), and were blowing mainly from N, NW, and S (63%).

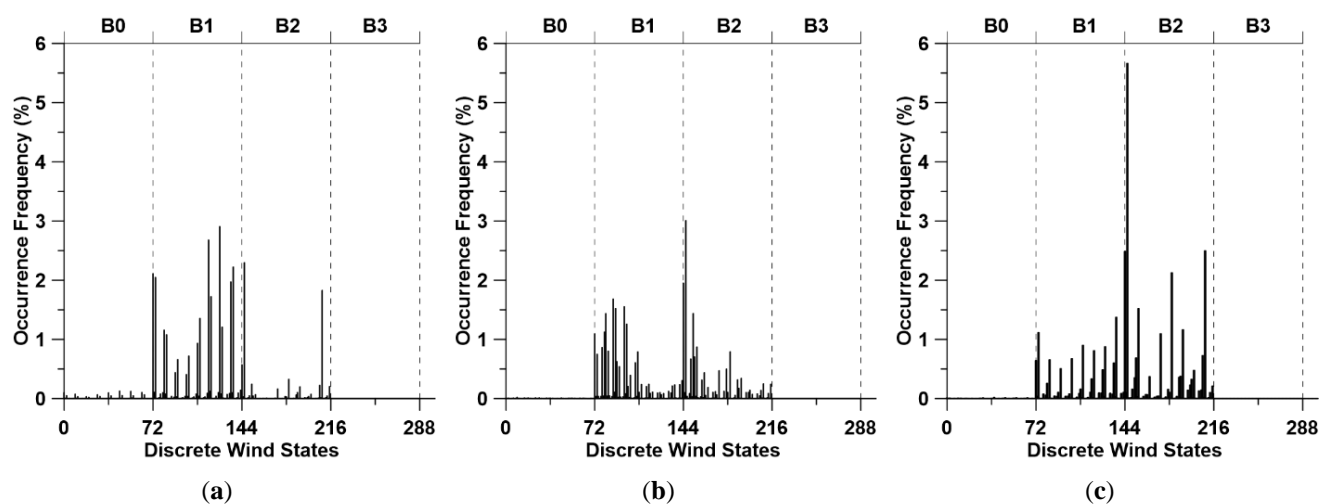


**Figure 8.** Occurrence frequencies of Mexico City discrete wind states. (a) 00-07 CST (early morning); (b) 08-15 CST (morning and early afternoon); and (c) 16-23 CST (late afternoon and night). Each frequency is the percentage of the number of times one discrete wind state was observed in the city, relative to the total number of wind events that occurred throughout the years 2001–2006.

**Table 9.** Absolute percentages of the wind events for discrete values of the wind parameters.

Time Period CST	WSP Beaufort Categories				Wind Direction								DIV < 0	VOR > 0
	B0	B1	B2	B3	N	NE	E	SE	S	SW	W	NW		
00-07	1	25	7	0	8	3	1	2	3	5	5	7	31	18
08-15	0	19	15	0	11	8	5	3	2	1	1	2	17	19
16-23	0	11	22	0	11	3	1	2	4	3	3	6	30	24
Total	1	55	44	0	30	14	7	7	9	9	9	15	78	61

In Table 10, the characteristics of the first ten highest frequency discrete wind states are described for each one of the 8 h periods. Early Morning (00-07 CST): the main wind states represent convergent low intensity winds (*light air*, in the Beaufort scale) blowing mainly from the N and NW (in average) with predominance of cyclonic vorticity. Morning and Early Afternoon (08-15 CST): the main wind states represent divergent, low intensity winds, blowing mainly from the N and NE (in average), with no predominance of any kind of vorticity. Late Afternoon and Night (16-23 CST): the main wind states represent winds with convergent and cyclonic features, blowing mainly from N and NW with speeds in the range of 1.5 to 3.5 m/s (*light breeze*, in the Beaufort scale).

### 3.3. Mexico City Wind Direction States (2001–2006)

Finally, a schematic view of the wind circulation in Mexico City is given by the WDSs that occurred in the city during the study period. Figure 9 shows the frequency distribution of the WDS. Table 11 summarizes the characteristics of the first 20 with the highest frequencies of occurrence.

**Table 10.** First ten highest frequency DWS for the time periods 00-07 CST (early morning), 08-15 CST (morning and early afternoon), and 16-23 CST (late afternoon and night).

Time Period	State ID	(U, $\theta$ , $\gamma$ , $\omega$ )	Frequency (%)	WSP (m/s)	WDR	$\gamma$	$\omega$
00-07 CST	126	(1, 6, 0, 0)	2.9077	$0.25 < v < 1.5$	W	Convergent	Anticyclonic
	117	(1, 5, 0, 0)	2.6776	$0.25 < v < 1.5$	SW	Convergent	Anticyclonic
	146	(2, 0, 0, 2)	2.2954	$1.5 < v < 3.5$	N	Convergent	Cyclonic
	137	(1, 7, 0, 2)	2.2231	$0.25 < v < 1.5$	NW	Convergent	Cyclonic
	72	(1, 0, 0, 0)	2.1109	$0.25 < v < 1.5$	N	Convergent	Anticyclonic
	74	(1, 0, 0, 2)	2.0462	$0.25 < v < 1.5$	N	Convergent	Cyclonic
	135	(1, 7, 0, 0)	1.9721	$0.25 < v < 1.5$	NW	Convergent	Anticyclonic
	209	(2, 7, 0, 2)	1.8276	$1.5 < v < 3.5$	NW	Convergent	Cyclonic
	119	(1, 5, 0, 2)	1.7230	$0.25 < v < 1.5$	SW	Convergent	Cyclonic
	110	(1, 4, 0, 2)	1.3559	$0.25 < v < 1.5$	S	Convergent	Cyclonic
08-15 CST	146	(2, 0, 0, 2)	3.0066	$1.5 < v < 3.5$	N	Convergent	Cyclonic
	144	(2, 0, 0, 0)	1.9512	$1.5 < v < 3.5$	N	Convergent	Anticyclonic
	87	(1, 1, 2, 0)	1.6811	$0.25 < v < 1.5$	NE	Divergent	Anticyclonic
	96	(1, 2, 2, 0)	1.5518	$0.25 < v < 1.5$	E	Divergent	Anticyclonic
	89	(1, 1, 2, 2)	1.5195	$0.25 < v < 1.5$	NE	Divergent	Cyclonic
	81	(1, 1, 0, 0)	1.4358	$0.25 < v < 1.5$	NE	Convergent	Anticyclonic
	152	(2, 0, 2, 2)	1.4358	$1.5 < v < 3.5$	N	Divergent	Cyclonic
	98	(1, 2, 2, 2)	1.2589	$0.25 < v < 1.5$	E	Divergent	Cyclonic
	80	(1, 0, 2, 2)	1.1239	$0.25 < v < 1.5$	N	Divergent	Cyclonic
	72	(1, 0, 0, 0)	1.0954	$0.25 < v < 1.5$	N	Convergent	Anticyclonic
16-23 CST	146	(2, 0, 0, 2)	5.6614	$1.5 < v < 3.5$	N	Convergent	Cyclonic
	209	(2, 7, 0, 2)	2.4970	$1.5 < v < 3.5$	NW	Convergent	Cyclonic
	144	(2, 0, 0, 0)	2.4874	$1.5 < v < 3.5$	N	Convergent	Anticyclonic
	182	(2, 4, 0, 2)	2.1261	$1.5 < v < 3.5$	S	Convergent	Cyclonic
	155	(2, 1, 0, 2)	1.5195	$1.5 < v < 3.5$	NE	Convergent	Cyclonic
	137	(1, 7, 0, 2)	1.3730	$0.25 < v < 1.5$	NW	Convergent	Cyclonic
	191	(2, 5, 0, 2)	1.1639	$1.5 < v < 3.5$	SW	Convergent	Cyclonic
	74	(1, 0, 0, 2)	1.1144	$0.25 < v < 1.5$	N	Convergent	Cyclonic
	173	(2, 3, 0, 2)	1.0954	$1.5 < v < 3.5$	SE	Convergent	Cyclonic
	110	(1, 4, 0, 2)	0.8995	$0.25 < v < 1.5$	S	Convergent	Cyclonic

In Figure 9, each WDS is identified by the decimal form of its octal ID. The x-axis is divided into 8 blocks; each one comprises the set of WDS for a given wind direction in the NE city quadrant (top axis). By its proper definition, the number of possible WDSs is 4096, but only the 66% of them were observed in the city in the period 2001–2006. The frequencies are expressed as percentages relative to the total number of wind events (52,584) in the study period. The scale of the y-axis has been set as logarithmic to facilitate the visualization of the smaller frequencies. As observed in Table 11, the occurrence frequency (5.92%) of WDS 0 (0000, northerly wind at all quadrants) is three times larger than WDS 7 (0007, northwesterly wind at SE quadrant, and northerly at other three) with the second-highest frequency (1.83%) and almost ten times larger than the WDS with the smallest frequency in this table.

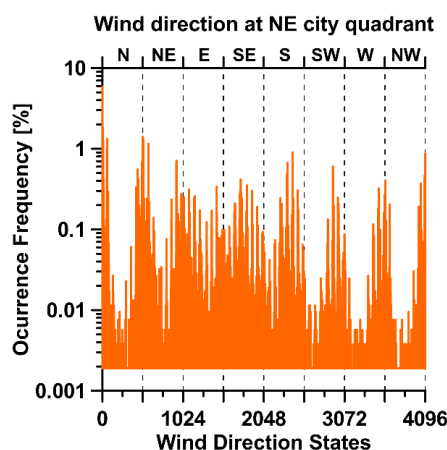


**Figure 9.** Occurrence frequencies of Mexico City wind direction states for the period of 2001–2006.

**Table 11.** First 20 highest frequency wind direction states occurred during the years 2001–2006

WDS (DEC)	WDS (OCT)	Events	Frequency (%)
0	0000	3111	5.92
7	0007	961	1.83
511	0777	740	1.41
1	0001	726	1.38
8	0010	718	1.37
63	0077	702	1.34
513	1001	695	1.32
521	1011	692	1.32
512	1000	640	1.22
9	0011	629	1.20
585	1111	607	1.15
56	0070	543	1.03
2412	4554	475	0.90
4095	7777	459	0.87
4094	7776	403	0.77
939	1653	377	0.72
504	0770	361	0.69
938	1652	353	0.67
2348	4454	351	0.67
510	0776	336	0.64

As a whole, the twenty wind direction states summarized in Table 11 make up the 26% of the total number of hourly model wind events. All the WDS presented in this table represent winds with a flow component from north in at least three of the city quadrants, with exception of the wind direction states identified by the octal numbers 4554, 1653, 1652, and 4454. The states 4554 and 4454 represent winds with a flow component from south, while the states 1653 and 1652 represent highly convergent winds toward the city's downtown (Figure 10).



**Figure 10.** The most frequent highly convergent WDS observed in Mexico City (2001–2006).

Tables 12–14 summarize the highest-frequency Mexico City wind direction states for the 00–07 CST, 08–15 CST, and 16–23 CST time periods. Each table shows the first fifteen WDS with the highest frequencies for one of the 8h-periods. These frequencies are relative to the total number of wind events in the study period.

**Table 12.** 00–07 CST.

WDS (D)	WDS (O)	FREQ (%)	WIND FLOW	
0	0000	0.8824	↓	↓
			↓	↓
939	1653	0.6903	→	↙
			↗	↖
938	1652	0.6504	→	↙
			↗	←
63	0077	0.6181	↓	↓
			↘	↘
511	0777	0.5933	↘	↓
			↘	↘
7	0007	0.5230	↓	↓
			↓	↘
4094	7776	0.4032	↘	↘
			↘	→
510	0776	0.3537	↘	↓
			↘	→
62	0076	0.3442	↓	↓
			↘	→
427	0653	0.3195	→	↓
			↗	↖
56	0070	0.3157	↓	↓
			↘	↓
1451	2653	0.3081	→	←
			↗	↖
4095	7777	0.2929	↘	↘
			↘	↘
428	0654	0.2872	→	↓
			↗	↖
940	1654	0.2872	→	↓
			↗	↑



**Table 13.** 08-15 CST.

WDS (D)	WDS (O)	FREQ (%)	WIND FLOW	
0	0000	2.6206	↓	↓
			↓	↓
8	0010	0.9490	↓	↓
			↙	↓
521	1011	0.8881	↓	↙
			↙	↙
9	0011	0.8805	↓	↓
			↙	↙
7	0007	0.8539	↓	↓
			↓	↘
585	1111	0.8044	↙	↙
			↙	↙
1	0001	0.5762	↓	↓
			↓	↙
512	1000	0.5268	↓	↙
			↓	↓
513	1001	0.4906	↓	↙
			↓	↙
522	1012	0.3537	↓	↙
			↙	←
520	1010	0.3423	↓	↙
			↙	↓
586	1112	0.3233	↙	↙
			↙	←
584	1110	0.2967	↙	↙
			↙	↓
1098	2112	0.2891	↙	←
			↙	←
1746	3322	0.2567	↖	↖
			←	←

In Table 12 (Early Morning), six wind direction states depict highly convergent winds (octal IDs: 1653, 1652, 0653, 2653, 0654, and 1654), seven describe winds with a westerly flow component at the western city quadrants (0077, 0777, 7776, 0776, 0076, 0070 and 7777), and the other two describe northerly winds (0007 and 0000). If we take into account that our lattice domain (Figure 2) is located relatively far from the eastern mountains (Sierra Nevada), all these states, excepting the last two, suggest katabatic winds blowing down from the surrounding mountains (mainly from Sierra las Cruces and Sierra Ajusco-Chichinautzin) towards the city [25,26]. In Table 13 (Morning and Early Afternoon), five of the wind direction states describe northerly winds (0000, 0010, 0007, 0001 and 1000), seven describe northeasterly winds (1011, 0011, 1111, 1001, 1010, 1112 and 1110), and the other three represent easterly winds (3322, 2112 and 1012). These WDSs represent the well-known Mexico City prevailing winds, which are mainly driven by the trade winds and the Caribbean low level jet [25–27]. The wind direction states in Table 14 (Late Afternoon and Night) describe winds blowing mainly from the north

(0000, 1001, 0070, 1000, 0001, 0007 and 0010), northwest (0777, 0077, 7777 and 0770), and northeast (1011 and 1111), although two of the states (4554 and 4454) correspond to winds blowing from S and SW. These WDS resemble the afternoon northerly and southerly gap winds [28] that are generated primarily by temperature differences between the basin and its surroundings, similar to the wind systems described by Kimura and Kuwagata [29]; however, because of the time period being considered, these WDSs could be representing gap winds superposed to katabatic winds.

**Table 14.** 16-23 CST.

WDS (D)	WDS (O)	FREQ (%)	WIND FLOW	
0	0000	2.4133	↓	↓
			↓	↓
511	0777	0.7055	↘	↓
			↘	↘
513	1001	0.6276	↓	↙
			↓	↙
56	0070	0.6066	↓	↓
			↘	↓
63	0077	0.5705	↓	↓
			↘	↘
512	1000	0.5553	↓	↙
			↓	↓
2412	4554	0.5325	↗	↑
			↗	↑
1	0001	0.5287	↓	↓
			↓	↙
4095	7777	0.5059	↘	↘
			↘	↘
7	0007	0.4507	↓	↓
			↓	↘
504	0770	0.3841	↘	↓
			↘	↓
2348	4454	0.3575	↑	↑
			↗	↑
8	0010	0.3385	↓	↓
			↙	↓
521	1011	0.3271	↓	↙
			↙	↙
585	1111	0.3233	↙	↙
			↙	↙

#### 4. Conclusions

A characterization of the Mexico City wind events of the period 2001–2006 was performed, including an estimation of their occurrence probabilities. The study was carried out under the lattice wind modeling approach at a meso- $\beta$  scale proposed by Salcido *et al.* [1] and Celada-Murillo *et al.* [3]. Hourly wind data from the meteorological network of the MCMA atmospheric monitoring system were used. The

systematic availability of high quality wind data from this network made it possible to perform studies for longer time periods with no additional technical problems. The conceptual simplicity of this analytic approach also allows its application for practical goals, such as identifying and selecting wind scenarios for air quality assessment [13,14] and wind resource assessment.

The data sets of the four wind state parameters follow statistics different from the normal distribution, as it is established by their values of skewness and kurtosis (both different from zero). The data sets of the wind velocity components and vorticity are peaked relative to a normal distribution, which is clearly reflected by their high kurtosis values, but kurtosis of wind divergence is low. The west-to-east wind velocity component (u) and vorticity are skewed right, while south-to-north wind velocity component (v) and wind divergence are skewed left. The basic statistics of the wind state parameters (Table 5) indicates that the data set closer to a normal distribution was that of wind divergence.

During early morning the prevailing winds were convergent (93%) with speeds from 0.25 to 1.5 m/s (75%), blowing mainly (75%) from N, NW, W and SW, and with a slight predominance (54%) of cyclonic vorticity. During morning and early afternoon a slight dominance of convergent winds (51%) was observed, the prevailing winds were blowing mainly (72%) from the N, NE and E, with speeds from 0.5 to 3.5 m/s, and revealed a slight predominance (57%) of cyclonic vorticity. During late afternoon and night, the prevailing winds were convergent (90%) and cyclonic (72%) with speeds from 1.5 to 3.5 m/s (66%), and blowing mainly (63%) from the N, NW, and S. Percentage figures are relative to the number of events in the 8h-period.

The set of Mexico City's wind direction states was obtained, the occurrence frequencies of the WDSs were estimated, and their arrangements according to the belonging of their occurrence hours to the time intervals of early morning, morning and early afternoon, and late afternoon and night were carried out. This analysis also permitted a schematic illustration of the principal wind circulation modes that prevailed in Mexico City during the period 2001–2006.

## Author Contributions

Salcido and Carreón-Sierra carried out the main part of writing, although all coauthors contributed to the text. The research was carried out by all co-authors, comprising both modelling work and also data analysis.

## Conflicts of Interest

The authors declare no conflict of interest.

## References

1. Salcido, A.; Celada-Murillo, A.T.; Castro, T. A meso- $\beta$  scale description of surface wind events in Mexico City during MILAGRO 2006 campaign. In Proceedings of the Second IASTED International Conference on Environmental Management and Engineering EME 2010; Canada, 15–17 July 2010.

2. Salcido, A.; Carreón-Sierra, S.; Celada-Murillo, A.T. A brief clustering analysis of the Mexico City local wind states occurred during the MILAGRO Campaign. In Proceedings of the 4th IASTED International Conference on Environmental Management and Engineering EME, Banff, AB, Canada, 16–17 July 2014.
3. Celada-Murillo, A.; Carreón-Sierra, S.; Salcido, A.; Castro, T.; Peralta, O.; Georgiadis, T. Main characteristics of Mexico City local wind events during the MILAGRO 2006 Campaign within a Meso- $\beta$  Scale Lattice Wind Modeling Approach. *ISRN Meteorol.* **2013**, doi:10.1155/2013/605210.
4. Dirección de Monitoreo Atmosférico de la Secretaría del Medio Ambiente (SEDEMA) del Gobierno del Distrito Federal. Available online: <http://www.aire.df.gob.mx/> (accessed on 23 May 2015).
5. Carreón-Sierra, S.; Salcido, A.; Castro, T.; Celada-Murillo, A.-T. Cluster analysis of the wind events and seasonal wind circulation patterns in the Mexico City region. *Atmosphere* **2015**, *6*, 1006–1031.
6. Ng, E.; Yuan, C.; Chen, L.; Ren, C.; Fung, J.C.H. Improving the wind environment in high-density cities by understanding urban morphology and surface roughness: A study in Hong Kong. *Landsc. Urban Plan.* **2011**, *101*, 59–74.
7. Matzarakis, A.; Mayer, H. Dependence of the thermal urban climate on morphological variables. *Ber. Meteor. Inst. Univ. Freiburg* **2008**, *17*, 129–139.
8. Oke, T.R. City size and the urban heat island. *Atmos. Environ.* **1973**, *7*, 769–779.
9. Jáuregui, E. Heat Island Development in Mexico City. *Atmos. Environ.* **1997**, *31*, 3821–3831.
10. Klaus, D.; Jáuregui, E.; Poth, A.; Stein, G.; Voss, M. Regular circulation structures in the tropical basin of México City as a consequence of the urban heat island effect. *Erdkunde* **1999**, *53*, 231–243.
11. Maignant, G.; Dutozia, J. Air pollution and urban morphology: A complex relation or how to optimize the pedestrian movement in town. In *Advanced Topics in Environmental Health and Air Pollution Case Studies*; Moldoveanu, A., Ed.; InTech: Rijeka, Croatia, 2011; pp. 197–208.
12. Weber, C.; Hirsch, J.; Ranchin, T.; Wald, L.; Ung, A.; Perron, G.; Kleinpeter, J. Urban morphology and atmospheric pollutants distribution. In Proceedings of the 23th International Symposium of the Urban Data Management Society, Prague, Czech Republic, 2–4 October 2002.
13. Peralta, O.; Castro, T.; Durón, M.; Salcido, A.; Celada-Murillo, A.T.; Navarro-González, R.; Márquez, C.; García, J.; de la Rosa, J.; Torres, R.; *et al.* H<sub>2</sub>S emissions from Cerro Prieto geothermal power plant, Mexico, and air pollutants measurements in the area. *Geothermics* **2013**, *46*, 55–65.
14. Salcedo, D.; Castro, T.; Ruiz-Suárez, L.G.; García-Reynoso, A.; Torres-Jardón, R.; Torres-Jaramillo, A.; Mar-Morales, B.E.; Salcido, A.; Celada, A.T.; Carreón-Sierra, S.; *et al.* Study of the regional air quality south of Mexico City (Morelos state). *Sci. Total Environ.* **2012**, *414*, 417–432.
15. Heller, E. Urban wind turbines. *Zoning Pract.* **2008**, *25*, 2–7.
16. Delgadillo-Polanco, V.M. Repopulation and rescuing of Mexico City's historic centre; a hybrid public action, 2001–2006. *Economía, Sociedad y Territorio* **2008**, *8*, 817–845. (in Spanish)
17. Gobierno del Distrito Federal. *Programa Integral de Transporte y Vialidad del Gobierno del Distrito Federal 2001–2006*; Gobierno del Distrito Federal: México City, Mexico, 2001.

18. Lozano, A.; Granados, F.; Torres, V.; Hernández, R.; Guzmán, A.; Alarcón, R.; Vargas, F.; Guarneros, L.; Argumedo, M.; Romero, E.; *et al.* *Simulación macroscópica del efecto de la “Fase I del proyecto Segundo Piso de Periférico y Viaducto” sobre el tráfico de la red vial de la Zona Metropolitana del Valle de México*; Gobierno del Distrito Federal: México City, Mexico, 2002.
19. Lozano, A.; Torres, V.; Guzmán, A.; Granados, F.; Álvarez-Icaza, L.; Magallanes, R.; Antón, J.P.; Luyando, G.; Vargas, F.; Argumedo, M.; *et al.* *Simulación macroscópica del efecto del “Proyecto Segundo Piso de Periférico y Viaducto” sobre el tráfico en la red vial de la Zona Metropolitana del Valle de México–Fase II*; Gobierno del Distrito Federal: México City, Mexico, 2002.
20. Gobierno del Distrito Federal. *Secretaría de Desarrollo Urbano y Vivienda (SEDUVI)*; Gobierno del Distrito Federal: México City, Mexico, 2007.
21. Salcido, A.; Celada-Murillo, A.T.; Villegas-Martinez, R.; Salas-Oviedo, H.; Sozzi, R.; Georgiadis, T. A micrometeorological data base for the Mexico City Metropolitan Area. *Nuovo Cim.* **2003**, *26C*, 317–355.
22. A detailed description of the MCMA-2003 field campaign is given at the web site of the Molina Center for Energy and the Environment. Available online: <http://www.mce2.org/en/field-campaigns/mcma-2003> (accessed on 24 July 2015).
23. Molina, L.T.; Madronich, S.; Gaffney, J.S.; Apel, E.; de Foy, B.; Fast, J.; Ferrare, R.; Herndon, S.; Jimenez, J.L.; Lamb, B.; *et al.* An overview of the MILAGRO 2006 campaign: Mexico City emissions and their transport and transformation. *Atmos. Chem. Phys.* **2010**, *10*, 8697–8760.
24. Shaefer, J.T.; Doswell, C.A., III. On the interpolation of a vector field. *Mon. Weather Rev.* **1979**, *107*, 458–476.
25. Jauregui, E. Local wind and air pollution interaction in the Mexico basin. *Atmósfera* **1988**, *1*, 131–140.
26. Klaus, D.; Poth, A.; Voss, M.; Jauregui, E. Ozone distributions in Mexico City using principal component analysis and its relation to meteorological parameters. *Atmósfera* **2001**, *14*, 171–188.
27. Muñoz, E.; Busalacchi, A.J.; Nigam, S.; Ruiz-Barradas, A. Winter and summer structure of the Caribbean low-level jet. *J. Clim.* **2008**, *21*, 1260–1276.
28. Doran, J.C.; Zhong, S. Thermally Driven Gap Winds into the Mexico City Basin. *J. Appl. Meteorol.* **2000**, *39*, 1330–1340.
29. Kimura, F.; Kuwagata, T. Thermally induced wind passing from plain to basin over a mountain range. *J. Appl. Meteorol.* **1993**, *32*, 1538–1547.